MEK inhibitor and anti-EGFR antibody overcome sotorasib resistance signals and enhance its antitumor effect in colorectal cancer cells

Cancer Letters. 2023; 567: 216264.

https://doi.org/10.1016/j.canlet.2023.216264

Nao Hondo, Masato Kitazawa, Makoto Koyama, Satoshi Nakamura, Shigeo Tokumaru, Satoru Miyazaki, Masahiro Kataoka, Kai Seharada and Yuji Soejima

Division of Gastroenterological, Hepato-Biliary-Pancreatic, Transplantation and Pediatric Surgery, Department of Surgery, Shinshu University School of Medicine, Matsumoto, Japan

Corresponding author: Masato Kitazawa, Division of Gastroenterological, Hepato-Biliary-Pancreatic, Transplantation and Pediatric Surgery, Department of Surgery, Shinshu University School of Medicine, 3-1-1 Asahi, Matsumoto, Nagano 390-8621, Japan. Phone: +81-263-37-2654; Fax +81-263-35-1282; E-mail: kita118@shinshu-u.ac.jp

Abstract

The Kirsten rat sarcoma (KRAS) oncogene was “undruggable” until sotorasib, a $KRAS^{G12C}$ selective inhibitor, was developed with promising efficacy. However, inhibition of mutant KRAS in colorectal cancer cells (CRC) is ineffective due to feedback activation of MEK/ERK downstream of KRAS. In this study, we screened for combination therapies of simultaneous inhibition to overcome sotorasib resistance using our previously developed Mix Culture Assay. We evaluated whether there was an additive effect of sotorasib administered alone and in combination with two or three drugs: trametinib, a MEK inhibitor, and cetuximab, an anti-epidermal growth factor receptor (EGFR) antibody. The MAPK pathway was reactivated in $KRAS^{G12C}$-mutated cell lines treated with sotorasib alone. Treatment with KRAS and MEK inhibitors suppressed the reactivation of the MAPK pathway, but upregulated EGFR expression. However, the addition of cetuximab to this combination suppressed EGFR reactivation. This three-drug combination therapy resulted in significant growth inhibition *in vitro* and *in vivo*. Our data suggest that reactive feedback may play a key role in the resistance signal in CRC. Simultaneously inhibiting KRAS, MEK, and EGFR is a potentially promising strategy for patients with $KRAS^{G12C}$-mutated CRC.

Keywords: Colorectal cancer, Kristen rat sarcoma 2 viral oncogene homolog, G12C, Sotorasib, Trametinib, Cetuximab

1. Introduction

Kirsten rat sarcoma (KRAS) is one of the most commonly mutated oncogenes in human cancers [1, 2]. KRAS protein normally functions as a molecular switch that cycles between an active state (GTP-bound form) and an inactive state (GDP-bound form) [3, 4]. Mutations in KRAS are found in approximately 40% of colorectal cancers (CRC) and typically occur at hotspots in codons 12, 13, and 61 [5-9]. These mutant KRAS proteins are in a constitutively GTP-binding active state and persistently activate downstream signals, including the RAF-MEK-ERK (MAPK) pathway, which enhances cell proliferation and survival [6,10,11]. Due to its high affinity for nucleotide and the lack of tractable binding pockets for small-molecule inhibitors, the therapeutic targeting of mutant KRAS has remained "undruggable" for more than three decades [4,12,13]. Recently, covalent inhibitors targeting a $KRAS^{G12C}$ mutation have been developed and shown promising efficacy in preclinical studies [14-16]. Two $KRAS^{G12C}$ inhibitors, sotorasib and adagrasib, have already entered clinical application. However, in clinical

55 trials, $KRAS^{G12C}$ inhibitors were not as effective against CRC as against non-small cell
56 lung cancer (NSCLC) [1, 5, 17]. In the phase 2 trial of sotorasib, the objective response
57 rate was 37.1% in NSCLC but 9.7% in CRC [5]. Another clinical trial of adagrasib
58 showed that the partial response rate and the duration of response were 53.3% and 16.4
59 months in NSCLC but 50% and 4.2 months in CRC, respectively, treated at the
60 recommended phase 2 dose [17].

61 Historically, resistance by feedback reactivation to single-agent therapies in
62 patients with CRC has been suggested. For example, due to feedback reactivation,
63 patients with CRC with $BRAF^{V600E}$ have limited sensitivity to a single-agent BRAF
64 inhibitor [18]. However, the simultaneous inhibition of epidermal growth factor receptor
65 (EGFR) and mitogen-activated protein kinase kinase (MEK) to suppress feedback
66 activation, in addition to BRAF inhibitors, can the enhance antitumoral effects [19-21].
67 Therefore, we hypothesized that a combination therapy targeting feedback reactivation
68 would overcome $KRAS^{G12C}$ inhibitors resistance in CRC.

69 In the present study, we screened for effective combination therapies for CRC
70 with $KRAS^{G12C}$. First, we assessed the feedback reactivation to $KRAS^{G12C}$ inhibition in
71 NSCLC and CRC cells. Next, we screened agents that would be effective in combination
72 therapy using Mix Culture Assays [22-24]. Furthermore, we evaluated the antitumor

effect of the combined inhibition of KRAS, EGFR, and MEK in CRC cells. This study demonstrates that the simultaneously inhibition of MEK and EGFR may overcome resistance signals to $KRAS^{G12C}$ inhibition and enhance the antitumoral effects both of *in vivo* and *in vitro*.

2. Materials and Methods

2.1. Cell culture

CACO-2 (wild-type KRAS, RRID: CVCL_0025) was purchased from RIKEN Cell Bank. SW48 (wild-type KRAS, RRID: CVCL_1724), SW1463 (KRAS G12C, RRID: CVCL_1718), NCI-H3122 (wild-type KRAS, RRID: CVCL_5160), and NCI-H358 (KRAS G12C, RRID: CVCL_1559) were purchased from the American Type Culture Collection (ATCC). Calu-1 (KRAS G12C, RRID: CVCL_0608), SW837 (KRAS G12C, RRID: CVCL_1729), and DLD-1 (KRAS G13A, RRID: CVCL_0248) were purchased from European Collection of Authenticated Cell Cultures (ECACC), Japanese Collection of Research Bioresources (JCRB) Cell Bank, and Cell Resource Center for Biomedical Research Institute of Development, Aging and Cancer, Tohoku University, respectively.

CACO-2 was maintained in a Dulbecco's modified Eagles medium (DMEM;

FUJIFILM Wako Pure Chemicals Corporation, Osaka, Japan). SW48 was maintained in RPMI-1640 with high glucose (FUJIFILM Wako Pure Chemicals Corporation). SW837, SW1463, and Calu-1 were maintained in DMEM/F12 (FUJIFILM Wako Pure Chemicals Corporation). DLD-1, NCI-H3122, and NCI-H358 were maintained in RPMI-1640 (FUJIFILM Wako Pure Chemicals Corporation). All cells were incubated with 10% fetal bovine serum (Biowest, Nuaillé, France) and 1% penicillin/streptomycin (FUJIFILM Wako Pure Chemicals Corporation) at 37 °C and 5% CO_2. All cells were routinely tested for *Mycoplasma* contamination using EZ-PCR™ Mycoplasma Detection Kit (Biological Industries, Beit Haemek, Israel.).

2.2. Antibodies and reagents

The following antibodies were used: Monoclonal mouse FLAG (#014-22383, RRID: AB_10660291; FUJIFILM Wako Pure Chemicals Corporation), monoclonal rabbit p-Erk1/2 (#4376, RRID: AB_331772; Cell Signaling Technology [CST], Danvers, MA, USA), monoclonal rabbit Erk1/2 (#4695, RRID: AB_390779; CST), monoclonal rabbit p-MEK1/2 (#9154, RRID: AB_2138017; CST), monoclonal rabbit MEK1/2 (#8727, RRID: AB_10829473; CST), monoclonal rabbit p-AKT (#4060, RRID: AB_2315049; CST), monoclonal rabbit AKT (#4691, RRID: AB_915783; CST),

monoclonal rabbit p-EGF Receptor (#3777, RRID: AB_2096270; CST), monoclonal rabbit EGF Receptor (#4267, RRID: AB_2246311; CST), monoclonal rabbit p-mTOR (#5536, RRID: AB_10691552; CST), monoclonal rabbit mTOR (#2972, RRID: AB_330978; CST), monoclonal mouse ribosomal s6 kinase (RSK; #sc-393147; Santa Cruz Biotechnology Santa Cruz, CA, USA), monoclonal mouse p-RSK (#sc-377526; Santa Cruz Biotechnology), β-actin (#sc-47778; Santa Cruz Biotechnology) , and Ki-76 (#SAB5700770; Sigma-Aldrich, St. Louis, MO, USA). The secondary antibodies used were polyclonal goat anti-mouse (#P0447; Dako, Agilent Technologies, Santa Clara, CA, USA) IgG and polyclonal goat anti-rabbit (#P0448; Dako, Agilent Technologies) IgG conjugated with HRP.

7-Aminoactinomycin D (7-AAD; #640912) was obtained from BioLegend, (San Diego, CA, USA). Sotorasib (AMG510), Adagrasib (MRTX849), RMC-4550, crizotinib, and gefitinib were purchased from Selleckchem (Houston, TX, USA). Trametinib and cobimetinib were purchased from Cayman Chemical (Ann Harbor, MI, USA). Cetuximab, panitumumab, and rapamycin were purchased from Merck KGaA (Darmstadt, Germany), Takeda Pharmaceutical Company (Tokyo, Japan), and Sigma-Aldrich, respectively.

2.3. Construction and retroviral transduction of KRAS mutations

Total mRNA content from CACO-2 cells was extracted using NucleoSpin RNAplus (#740984; Takara Bio, Shiga, Japan), and cDNA was synthesized using PrimeScript RT Master Mix from the PrimeScript™ RT reagent kit (#RR037; Takara Bio). KRAS-4B carrying a C-terminal FLAG was amplified using PCR with PrimeSTAR® Max DNA Polymerase (#R045; Takara Bio) using CACO-2 cDNA as a template. The amplified KRAS-4B was inserted into the pMXs-IRES-GFP vector using the In-Fusion® HD Cloning kit (#639649; Takara Bio) by the inverse PCR method. Next, the pMXs-IRES-GFP vector carrying the KRAS wild-type gene was used as a template to create vectors carrying the KRAS mutations (G12C and G12D) with C-termed FLAG using the In-Fusion® HD Cloning kit by the inverse PCR method. Then, using the pMXs-IRES-GFP (wild-type KRAS, G12C, and G12D) vectors as a template, pDON-5 Neo DNA vectors (Takara Bio) carrying the wild-type KRASgene and its mutations were constructed using the In-Fusion® HD Cloning kit by the inverse PCR method. The DNA sequences of all the constructs were confirmed using ABI 3130xl Genetic Analyzer using BigDye® Terminator v3.1 Cycle Sequencing Kit (#4337454; Thermo Fisher Scientific, Waltham, MA, USA). These vectors were transfected into amphotropic packaging cells Phoenix-AMPHO (ATCC) using PEI MAX (Polysciences, Inc., Warrington, PA, USA) for retroviral transduction. The virus-containing supernatants were harvested 24 and 48 h

after gene transduction, and CACO-2 and SW48 cells were infected with the retroviral particles on plates coated with RetroNectin (#T100; Takara Bio). The transduction efficiency of pMXs-IRES-GFP vectors was confirmed using the GFP-positive ratio as measured using a flow cytometer (BD FACSCanto II; BD Biosciences, Franklin Lakes, NJ, USA) and analyzed with Kaluza 2.1 software (Beckman Coulter, Brea, CA, USA). The following transduction using pDON-5Neo DNA vectors, the transduced cells were selected via culture with G418 for 10 d. The transduction efficiency of pDON-5Neo DNA vectors was confirmed using western blotting. The methods of creating these vectors and retroviral transduction are shown in the paper by Koyama et al. [22].

2.4. Cell proliferation assay

Cell proliferation was measured using a Cell Counting Kit-8 (CCK-8) (#343-07623; Dojindo Laboratories, Kumamoto, Japan). Cells (5.0×10^3/well) were seeded into a 96-well tissue culture plate and incubated at 37 °C. After 16 h of incubation, each agent (sotorasib 1 to 10^5 nmol/L, trametinib 1 nmol/L, and cetuximab 5 µg/mL) or DMSO was added to the cells. Following 24 or 72 h, the CCK8 reagent (10 µl/well) was added and incubated at 37 °C for 2 h. Absorbance was measured using a plate reader at 450 nm, and cell viability was calculated as relative values from DMSO absorbance. The data are

representative of three independent experiments in triplicate.

2.5. Protein sample preparation and western blotting

After seeding and drug treatment, cells were washed with cold phosphate-buffered saline and lysed in RIPA Lysis Buffer System (#sc-24948; Santa Cruz Biotechnology) on ice for 30 min. Lysates were separated by centrifugation at 10,000 × g for 10 min at 4 °C, and the resultant supernatant was collected as the total cell lysate. Protein was quantified using a Pierce BCA Protein assay kit (#23227; Thermo Fisher Scientific), and 10–15 μg of protein was separated using NuPage 4-12% gel (# NP0322; Thermo Fisher Scientific) and then electroblotted onto a PVDF membrane. The membrane was blocked with Tris-buffered saline containing 5% non-fat dry milk and 0.1% Tween-20 for 1 h at room temperature and then probed using the primary antibodies at 4 °C for 16 h. The membrane was then incubated with horseradish peroxidase-conjugated secondary antibody for 1 h at room temperature, which was detected by enhanced chemiluminescence using Immobilon Western HRP (Amersham ECL Prime Western Blotting Detection Reagent; #RPN2236; Cytiva, Marlborough, UK). The density of the target protein measured using Image Lab Software version 6.0.1 (Bio-Rad Laboratories, Hercules, CA, USA) was divided by the density of each β-actin band to

obtain the actual density.

2.6. Mix Culture assay

We have previously developed and reported a Mix Culture Assay for the stable and reliable screening of effective therapeutic targets, using the pMXs-IRES-GFP vector and measured by a flow cytometer. The outline of this experimental system, the calculation method for the relative proliferation ratio (RPR), and the experimental example are shown in our previous report [22-24]. Wild-type and mutant KRAS genes (G12C and G12D) were inserted into CACO-2 cells using the pMX-IRES-GFP vector for this assay. High gene transduction efficiency of ≥90% was obtained as determined by the GFP-positive rate (%) measured using a flow cytometer. After gene transfer, GFP expression in gene-transduced cells stabilizes at approximately 7 passages; therefore, cells with 7–10 passages were used. Parental cells (GFP-negative) and gene-transduced cells (GFP-positive) were mixed at an ideal 1:1 ratio. At it is not possible to maintain the GFP-positive rate constant at 50%, an acceptable range of 50% ±10% is considered acceptable. On the first day, the mixed cells were seeded at 20% confluency into a 12-well plate and cultured for 12 d with the targeting agents. They were then passaged at a 5:1 ratio before reaching confluence. On d 12, the cells were harvested and stained with

7-AAD. The population that was 7-AAD-negative, representing viable cells, was gated, and the GFP-positive ratio of these populations was determined using a flow cytometer. We calculated the RPR using the following formula, d 0 GFP-positive rate (%) (A) and d 12 GFP-positive rate (%) (B). RPR=B(100-A)/A(100-B). A low RPR indicated that the GFP-positive cell population was sensitive to the drug, whereas a high RPR indicated drug resistance. Using this system, we evaluated the drug sensitivities of KRAS-transduced cells to several molecular-targeting drugs.

2.7. Establishment of sotorasib-resistant cells

Sotorasib-resistant cells were established by exposure of $KRAS^{G12C}$-induced CACO-2 cells to increasing concentrations of sotorasib. The initial concentration of sotorasib was 50 nM. When the cells adapted to the drug, the concentration of sotorasib was gradually increased by 1.5 to 2 times every week to a final concentration of 1 μM.

2.8. In vivo xenograft experiments

All animal experiments were carried out in compliance with the Guide for the Care and Use of Laboratory Animals (eighth Edition) and approved by the Institutional Animal Care and Use Committee with Shinshu University (Matsumoto, Japan; approval

no. 020085). Male 6–8-week-old BALB/c nude mice (weight, 23–27 g) were purchased from CLEA Japan (Shizuoka, Japan). The total number of mice used throughout was n=52. Mice were maintained in a specific pathogen-free room with a 12-h light/dark cycle and free access to water and food. For the reagent experiment, xenograft tumors were generated via the subcutaneous injection of CACO-2 cells (5×10^6) stably expressing wild-type, G12C or G12D mutant KRAS in a 200 μL solution [50% Hank's Balanced Salt Solution (FUJIFILM Wako Pure Chemicals Corporation) + 50% Matrigel (Corning, Inc., Corning, NY, USA)] into the flanks of mice. Vehicle (12.5% Cremophor, 12.5% ethanol, 75%), sotorasib (0.5 mg/kg), and/or trametinib (0.1 mg/kg) were orally administered once daily for 21 consecutive days to mice (n=4 per group) when tumor size reached 100–200 mm^3. Cetuximab (50 mg/kg) was intraperitoneally administered once a week. The tumor volume was measured twice weekly according to the following formula: Volume (mm^3) = 0.5× $width^2$ (mm) × length (mm). All mice were sacrificed by cervical dislocation under 3% sevoflurane anesthesia on d 23.

2.9. Immunohistochemistry (IHC)

The resected xenograft tumors were fixed in 4% paraformaldehyde for 16 h at room temperature and embedded in paraffin, and then tissue sections (4 μm) were prepared.

235 Antigen retrieval was performed by boiling the sections at 98˚ °C for 25 min in 1 mM
236 EDTA2Na solution (pH 9.0). The slides were then subjected to endogenous peroxidase
237 blocking with 3% H_2O_2. The primary antibodies were added to the slides, which were
238 incubated for 16 h at 4 °C in a humidified chamber. Subsequently, the slides were
239 visualized using the Histofine Simplestain Max PO kit (cat. no. 414142F; Nichirei
240 Bioscience, Tokyo, Japan) for 1 h at room temperature. HRP-conjugated streptavidin was
241 used to attach peroxidase to the antibodies, and DAB chromogen was used for
242 visualization. Then, hematoxylin was used for nuclear counterstaining for 30 s at room
243 temperature.
244
245 ***2.10. Statistical analysis***
246 All statistical analyses were performed with EZR (Saitama Medical Center, Jichi
247 Medical University, Saitama, Japan) [25], which is a graphical user interface for R (The
248 R Foundation for Statistical Computing, Vienna, Austria, version 1.51). More precisely,
249 it is a modified version of R commander (version 2.6-2) designed to add statistical
250 functions frequently used in biostatistics. Statistical significance was evaluated using an
251 unpaired Student's t-test or one-way analysis of variance followed by Bonferroni's
252 correction. All error bars represent means with standard error of the mean. Values with

253 $P<0.05$ was considered statistically significant.

254

255

256 **3. Results**

257 ***3.1 Feedback reactivation of the RAS/MAPK pathway occurs following treatment with***

258 ***sotorasib in CRC lines***

259 To understand the mechanistic basis for differential clinical responses to

260 treatment with the selective $KRAS^{G12C}$ inhibitor sotorasib in CRC and NSCLC, we

261 analyzed the effect of this drug in a panel of cell lines with wild-type KRAS, $KRAS^{G12C}$

262 mutations, and other mutations (Fig. 1A). Response to sotorasib was measured in a dose-

263 response cell proliferation assay. Sotorasib inhibited the proliferation of cells with the

264 $KRAS^{G12C}$ but not that of cells with wild-type KRAS or other type mutations. However,

265 at high concentrations (5 μM), the antiproliferative effects of sotorasib were more

266 pronounced in NSCLC cells than in CRC cells (Table S1).

267 We then explored the potential role of feedback reactivation under of KRAS

268 inhibition. NSCLC (NCI-H358 and Calu-1) and CRC cell lines (SW837 and SW1463)

269 with the $KRAS^{G12C}$ mutation and those with wild-type KRAS (NCI-H3122 and DLD-1)

270 were treated with sotorasib, and eedback reactivation was assessed at different time points

after treatment (4–24 h). In both NSCLC and CRC cell lines with the $KRAS^{G12C}$ mutation, the expressions of pERK and pAKT were suppressed at 4 h of exposure to sotorasib. However, after 24 h of treatment, the expression of pERK remained suppressed in NSCLC cell lines but was increased in CRC cell lines (Fig. 1B). These data suggest the resistance to sotorasib in CRC cells corresponded with feedback reactivation, particularly the reactivation of the MAPK pathway.

To identify the impact of KRAS mutations on feedback reactivation following $KRAS^{G12C}$ inhibition in CRC, we assessed the effects of sotorasib using KRAS gene-transduced CRC cells. Transduction of wild-type or mutant KRAS genes were confirmed using an anti-FLAG antibody (Fig. 2A), KRAS-transduced cells were treated with sotorasib, and the MAPK pathway was investigated. MAPK pathway was suppressed after 4 h of exposure to sotorasib in $KRAS^{G12C}$ transduced cells, but not in cells transduced with the wild-type KRAS nor $KRAS^{G12D}$ genes. Feedback reactivation of MAPK was also observed in only $KRAS^{G12C}$ transduced cells after 24 h of sotorasib exposure (Fig. 2B, C). The PI3K/AKT pathway was not affected by sotorasib in this model. This result indicates that KRAS-mutation-transduced CRC cells showed the same feedback reactivation as KRAS-mutant CRC cell lines. Furthermore, these data also suggest that inhibiting the feedback reactivation of the MAPK pathway could enhance

289 the efficacy of sotorasib.

290

291 ***3.2. Screening for combination therapy with sotorasib using mix culture assay***

292 We further evaluated the drug sensitivities of KRAS-transduced CRC cells. We
293 have previously developed and reported a mix culture assay for the stable and reliable
294 screening of effective therapeutic targets [22-24]. In the present study, parental cells
295 (GFP-negative) and KRAS gene-transduced cells (GFP-positive) were mixed and treated
296 for 12 d, and drug sensitivity was evaluated by changes in the positive rate of GFP. First,
297 the drug sensitivities to $KRAS^{G12C}$ inhibitors were evaluated (Fig. 3A) and the results
298 showed that RPR was only significantly reduced in G12C. This result indicates that the
299 effects of sotorasib and adagrasib are selective for $KRAS^{G12C}$ mutation and do not cross-
300 react with other KRAS mutations, which is consistent with the results reported by
301 Kitazawa et al. [24]. Next, we evaluated the combined effect of sotorasib with several
302 molecular-targeting agents for the screening of effective treatments. The combination of
303 the MEK inhibitor, trametinib, and cobimetinib, significantly enhanced the RPR-lowering
304 effect of sotorasib in G12C (Fig. 3B). Anti-EGFR antibodies, cetuximab, and
305 panitumumab, induced a significantly high RPR in cells with KRAS mutations in a dose-
306 dependent manner, indicating that KRAS mutations led to resistance to EGFR inhibitors

(Fig. 3C), as previously reported [22]. The combination of sotorasib with anti-EGFR antibodies alleviated the resistance to anti-EGFR antibodies in $KRAS^{G12C}$-induced cells. The plots of the flow cytometry analysis are shown in Supplementary Fig. S1. No other agents targeting FGF/FGFR, mTOR/AKT, and ALK/ROS1/MET signals showed concomitant effects with sotorasib (Fig. S2). Based on these results, we investigated the efficacy of the combination therapy of sotorasib, MEK inhibitor, and anti-EGFR antibody.

3.3. MEK inhibitor and anti-EGFR antibodies enhance the efficacy of sotorasib

We evaluated the resistance signal of sotorasib and the efficacy of the combined use of the MEK inhibitor and/or anti-EGFR antibodies in $KRAS^{G12C}$-induced cells. KRAS gene-transduced cells were treated with sotorasib, trametinib, and/or cetuximab for 24 h, followed by analysis of the EGFR and RAS/MAPK pathways by western blot analysis (Fig. 4A). A single treatment with sotorasib for 24 h increased the protein expression of in pMEK and pERK. However, pERK remained suppressed in cells receiving the combination treatment of sotorasib and trametinib, whereas the expression of pEGFR was upregulated. Notably adding cetuximab suppressed the reactivation of EGFR. Next, cell proliferation was measured by a CCK-8 assay (Fig. 4B). Consistent with the mix culture assay results, sotorasib showed a specific inhibition effect on

KRAS^{G12C}-induced cells. KRAS^{G12C}-transduced cells showed resistance to treatment with cetuximab, which was alleviated by the combination treatment with sotorasib. The comparison of treatment with sotorasib alone vs. sotorasib plus trametinib or sotorasib plus cetuximab showed a more pronounced inhibitory effect with the two-drug combination;however, the difference was not significant. In contrast, the combination of the three drugs showed a significantly more inhibitory effect on the growth of KRAS^{G12C}-induced cells compared to treatment with sotorasib alone.

Next, we established sotorasib-resistant CRC cells using KRASG12C-induced cell lines. The sensitivity of non-resistant and resistant cell lines to sotorasib is shown in Supplementary Fig. S3. We evaluated the effect of the combination therapy on EGFR and RAS/MAPK signaling and the proliferation of resistant cells. Although stronger reactivation of pERK was observed in sotorasib-resistant cells, the three-drug combination therapy suppressed pERK reactivation in resistant cells (Fig. 4C). The CCK-8 assay revealed that sotorasib alone had no inhibitory effect on cell proliferation, whereas the combination of trametinib or cetuximab showed some inhibition, and the combination of three drugs showed a more pronounced inhibition on cell proliferation (Fig. 4D).

3.4. Combination therapy of sotorasib, trametinib, and cetuximab is effictive in vivo

We generated murine xenografts from KRAS-transduced CACO-2 cells and investigated sotorasib efficacy *in vivo*. Similar to the *in vitro* results, a single-agent use of 1 mg/kg/day of sotorasib showed selective antitumor effects on $KRAS^{G12C}$ mutated cells only (Fig. 5A). We then evaluated whether there was an additive effect of sotorasib administered alone and in combination with two or three drugs: trametinib, a MEK inhibitor, and cetuximab, an anti-EGFR antibody drug. The dose of sotorasib was reduced to 0.5 mg/kg/day, and the doses of trametinib and cetuximab were set to doses that did not show tumor growth inhibition alone in this xenograft model. Notably, in this *in vivo* study, the two-drug combinations of sotorasib plus trametinib and sotorasib plus cetuximab showed significant growth inhibition effects compared to sotorasib alone, and the three-drug combination showed significant inhibition versus those two-drug combinations (Fig. 5B). The expression of pERK was induced by treatment with sotorasib alone whereas the three-drug combination suppressed pERK expression and reduced the number of Ki-67 positive cells (Fig. 5C). More importantly, the three-drug combination induced significantly massive tumor shrinkage in xenografts with $KRAS^{G12C}$ mutated tumors without reducing the body weight of mice. The fluctuation in body weight was within 10% in all mice throughout the experiments (Fig. S4).

4. Discussion

Recently developed covalent $KRAS^{G12C}$ inhibitors have shown promising efficacy in patients with $KRAS^{G12C}$ mutation in phase 1–2 clinical trials; however, these reports showed substantial differences in the response rate between patients with NSCLC and CRC [1, 5, 17]. In the present study, we demonstrated that reactivation of the MAPK pathway and EGFR occurred following treatment with $KRAS^{G12C}$ inhibitors in CRC cells. Furthermore, combined treatment of MEK inhibitors and anti-EGFR antibodies enhanced the antitumor effect of the $KRAS^{G12C}$ inhibitor both *in vivo* and *in vitro*. Previous efforts on a single agent to target the RAS/RAF/MEK pathway have shown poor efficacy in patients with CRC. For example, $BRAF^{V600E}$ cancers, one of the driver oncogene mutations of the RAS/RAF/MAPK pathway, were treated with a BRAF inhibitor. The inhibitor showed promising efficacy in single-agent therapy against many cancers, such as melanoma and NSCLC, but was not as effective in patients with CRC [18]. These resistances in CRC are considered to correspond to adaptive feedback reactivation [21, 26]; when BRAF was inhibited, ERK-dependent negative feedback mediators were reduced, and the MAPK pathway was reactivated by the activation of other RAF kinases, such as CRAF, in patients with CRC. Clinically, the simultaneous inhibition of BRAF,

379 MEK, and EGFR is effective in patients with CRC with $BRAF^{V600E}$ [19, 21]. This
380 adaptive feedback also may lead to therapeutic resistance to treatment with $KRAS^{G12C}$
381 inhibitors in patients with CRC. Previous studies reported rebound activation of the
382 MAPK pathway was observed in CRC cells under $KRAS^{G12C}$ inhibition [27, 28] and
383 suggested this feedback reactivation was induced by the activation of EGFR and other
384 RAS, such as NRAS and HRAS. These reports also showed that the vertical inhibition of
385 factors upstream of RAS, such as EGFR and SHP-2 suppresses feedback reactivation and
386 shows a stronger antitumor effect than a single treatment.

387 In this study, we screened for effective co-target inhibition to overcome the
388 resistance feedback reactivation induced by $KRAS^{G12C}$ inhibition using a unique and
389 useful screening procedure: Mix Culture Assay [22, 24]. Our data indicated that the
390 combined inhibition of KRAS with MEK showed a stronger inhibitory effect on CRC
391 proliferation than single KRAS inhibition or in combination with other RTK inhibitors.
392 We also found that cells with KRAS mutations showed resistance to anti-EGFR
393 antibodies, as reported by Koyama et al. [22], which was alleviated by the combination
394 treatment with KRAS inhibitor in cells with the $KRAS^{G12C}$ mutation. Moreover, the
395 simultaneous inhibition with KRAS, MEK, and EGFR inhibitors suppressed the
396 proliferation of CRC cells more effectively than single or two-drug therapy *in vivo*. The

397 combination therapy also effectively inhibited the proliferative activity of resistant cell
398 lines, suggesting that it may overcome the real-world problem of drug resistance
399 acquisition. Notably, the combination of the three drugs at the doses used in this study did
400 not induced weight loss in mice. Furthermore, as these agents have been previously used
401 in clinical practice, this three-drug combination therapy is expected to be a feasible
402 treatment in humans and could be a promising therapeutic strategy in the near future.

403 In addition, drug resistance could occur by other mechanisms, such as a gain of
404 a stem cell-like state. Cancer stem cells have been associated with the development of
405 CRCs, drug resistance, recurrence, and metastasis [29, 30]. In this study, although we did
406 not analyze the effect of stem cells, we revealed that the resistance signal associated with
407 the EGFR and RAS/MAPK pathways was overcome by the upstream vertical inhibition.
408 In addition, we did not investigate the effect of the tumor microenvironment because our
409 study was limited to xenograft models using nude mice. Therefore, there might be
410 additional signaling from tumor stroma that activates other signals in cancer cells, which
411 should be investigated in future studies.

412 The present study suggests that vertical inhibition of the target single-RTK
413 pathway can effectively overcome the resistance feedback reactivation induced by
414 KRAS inhibitors in CRC [27, 28]. These results provide important insights into the

development of treatments for other KRAS mutations. In CRC, KRAS mutations frequently occur in G12D (28–34%), G12V (17–18%), and G13D (18–20%), and less frequently in G12C (5–10%) [9, 31, 32]. Recently, a selective, noncovalent inhibitor targeting $KRAS^{G12D}$ mutation, MRTX1133, has been developed [33]. MRTX1133 showed a promising antitumor effect in $KRAS^{G12D}$ pancreatic cells *in vitro* and *in vivo.* Although clinical trials with different $KRAS^{G12D}$ inhibitors are expected, resistance similar to $KRAS^{G12C}$ inhibitors in CRC might still occur. Nevertheless, a simultaneous vertical inhibition targeting feedback reactivation would be an effective treatment in patients with CRC, despite resistance to KRAS inhibitors.

Patients with CRC with KRAS mutation have a poor prognosis because anti-EGFR antibodies are ineffective against KRAS-mutated cells [7, 8]. However, our data showed that combining EGFR inhibitors with $KRAS^{G12C}$ inhibitors can alleviate the resistance of KRAS-mutated cells to anti-EGFR antibodies. In KRAS-mutant CRC, mutant KRAS is continuously active, promoting the proliferation of tumor cells. Inhibition of mutant KRAS leads to the suppression of stimulation to RTKs. Thus, we observed an antitumor effect of anti-EGFR antibodies on $KRAS^{G12C}$ mutant CRC cells in combination with KRAS and MEK inhibitors. Combination therapy with mutant-KRAS inhibitors, MEK inhibitors, and anti-EGFR antibodies to suppress adaptive feedback

reactivations is expected to significantly improve the prognosis of patients with CRC with mutant KRAS with drug resistance and poor prognosis. Similar to how anti-EGFR antibodies have dramatically improved the prognosis of CRC with wild-type KRAS, combination therapy based on mutant-KRAS inhibitors may revolutionize the treatment of CRC with KRAS mutations. Furthermore, therapeutic strategies targeting other gene mutations in CRC may also be effective.

5. Conclusion

This study suggests that feedback reactivation of the MAPK pathway and EGFR may play a key role in the resistance signal to sotorasib in CRC, and that the combination of MEK inhibitors and anti-EGFR antibodies with sotorasib may overcome this resistance signal and enhance the antitumoral effects against CRC. This three-drug combination therapy may become a promising strategy for patients with $KRAS^{G12C}$-mutated CRC.

Acknowledgments

This work was supported by the Japan Society for the Promotion of Science KAKENHI (grant no. JP22K15555, to M. Kitazawa) and the Japanese Foundation for Multidisciplinary Treatment of Cancer (JFMC2020; no Grant Number, to M. Kitazawa).

We would like to thank Editage (www.editage.com) for English language editing.

Data availability

The data generated in this study are available within the article and its supplementary data files.

References

[1] Hong DS, Fakih MG, Strickler JH, Desai J, Durm GA, Shapiro GI, *et al.* $KRAS^{G12C}$ inhibition with sotorasib in advanced solid tumors. *N Engl J Med* **2020**;383:1207–17.

[2] Simanshu DK, Nissley DV, McCormick F. RAS proteins and their regulators in human disease. *Cell* **2017**;170:17–33.

[3] Ryan MB, Corcoran RB. Therapeutic strategies to target RAS-mutant cancers. *Nat Rev Clin Oncol* **2018**;15:709–20.

[4] Awad MM, Liu S, Rybkin II, Arbour KC, Dilly J, Zhu VW, *et al.* Acquired resistance to $KRAS^{G12C}$ inhibition in cancer. *N Engl J Med* **2021**;384:2382–93.

[5] Fakih MG, Kopetz S, Kuboki Y, Kim TW, Munster PN, Krauss JC, *et al.* Sotorasib for previously treated colorectal cancers with KRASG12C mutation (CodeBreaK100): A prespecified analysis of a single-arm, phase 2 trial. *Lancet Oncol*

2022;23:115–24.

[6] Schubbert S, Shannon K, Bollag G. Hyperactive Ras in developmental disorders and cancer. *Nat Rev Cancer* **2007**;7:295–308.

[7] Karapetis CS, Khambata-Ford S, Jonker DJ, O'Callaghan CJ, Tu D, Tebbutt NC, *et al.* K-ras Mutations and benefit from cetuximab in advanced colorectal cancer. *N Engl J Med* **2008**;359:1757–65.

[8] Amado RG, Wolf M, Peeters M, Van Cutsem E, Siena S, Freeman DJ, *et al.* Wild-type KRAS is required for panitumumab efficacy in patients with metastatic colorectal cancer. *J Clin Oncol* **2008**;26:1626–34.

[9] Imamura Y, Lochhead P, Yamauchi M, Kuchiba A, Qian ZR, Liao X, *et al.* Analyses of clinicopathological, molecular, and prognostic associations of KRAS codon 61 and codon 146 mutations in colorectal cancer: Cohort study and literature review. *Mol Cancer* **2014**;13:135.

[10] Cully M. Downward J. SnapShot: Ras Signaling. *Cell* **2008**;133:1292–1292.e1.

[11] Vetter IR, Wittinghofer A. The guanine nucleotide-binding switch in three dimensions. *Science* **2001**;294:1299–304.

[12] Papke B, Der CJ. Drugging RAS: Know the enemy. *Science* **2017**;355:1158–63.

[13] Moore AR, Rosenberg SC, McCormick F, Malek S. RAS-targeted therapies: Is the

undruggable drugged? *Nat Rev Drug Discov* **2020**;19:533–52.

[14] Patricelli MP, Janes MR, Li LS, Hansen R, Peters U, Kessler LV, *et al.* Selective inhibition of oncogenic KRAS output with small molecules targeting the inactive state. *Cancer Discov* **2016**;6:316–29.

[15] Janes MR, Zhang J, Li LS, Hansen R, Peters U, Guo X, *et al.* Targeting KRAS mutant cancers with a covalent G12C-specific inhibitor. *Cell* **2018**;172:578–589.e17.

[16] Fell JB, Fischer JP, Baer BR, Ballard J, Blake JF, Bouhana K, *et al.* Discovery of tetrahydropyridopyrimidines as irreversible covalent inhibitors of KRAS-G12C with in vivo activity. *ACS Med Chem Lett* **2018**;9:1230–4.

[17] Ou S-HI, Jänne PA, Leal TA, Rybkin II, Sabari JK, Marve MA. First-in-human phase I/IB dose-finding study of adagrasib (MRTX849) in patients with advanced $KRAS^{G12C}$ solid tumors (KRYSTAL-1). *J Clin Oncol* **2022**;40:2530–8.

[18] Hyman DM, Puzanov I, Subbiah V, Faris JE, Chau I, Blay JY, *et al.* Vemurafenib in multiple nonmelanoma cancers with BRAF V600 mutations. *N Engl J Med* **2015**;373:726–36.

[19] Kopetz S, Grothey A, Yaeger R, Van Cutsem E, Desai J, Yoshino T, *et al.* Encorafenib, binimetinib, and cetuximab in BRAF V600E–mutated colorectal cancer. *N Engl J Med* **2019**;381:1632–43.

505 [20] Corcoran RB, Atreya CE, Falchook GS, Kwak EL, Ryan DP, Bendell JC, *et al.*
506 Combined BRAF and MEK inhibition with dabrafenib and trametinib in BRAF
507 V600-Mutant colorectal cancer. *J Clin Oncol* **2015**;33:4023–31.
508 [21] Corcoran RB, André T, Atreya CE, Schellens JHM, Yoshino T, Bendell JC, *et al.*
509 Combined BRAF, EGFR, and MEK inhibition in patients with $BRAF^{V600E}$ -mutant
510 colorectal cancer. *Cancer Discov* **2018**;8:428–43.
511 [22] Koyama M, Kitazawa M, Nakamura S, Matsumura T, Miyazaki S, Miyagawa Y, *et*
512 *al.* Low-dose trametinib and Bcl-xL antagonist have a specific antitumor effect in
513 KRAS-mutated colorectal cancer cells. *Int J Oncol* **2020**;57:1179–91.
514 [23] Kitazawa M, Hida S, Fujii C, Taniguchi S, Ito K, Matsumura T, *et al.* ASC induces
515 apoptosis via activation of caspase-9 by enhancing gap junction-mediated
516 intercellular communication. *PLOS ONE* **2017**;12:e0169340.
517 [24] Kitazawa M, Miyagawa Y, Koyama M, Nakamura S, Hondo N, Miyazaki S, *et al.*
518 Drug sensitivity profile of minor KRAS mutations in colorectal cancer using mix
519 culture assay: The effect of AMG-510, a novel KRAS G12C selective inhibitor, on
520 colon cancer cells is markedly enhanced by the combined inhibition of MEK and
521 BCL-XL. *Mol Clin Oncol* **2021**;15:148.
522 [25] Kanda Y. Investigation of the freely available easy-to-use software ‘EZR’ for

medical statistics . *Bone Marrow Transplant* **2013**;48:452–8.

[26] Corcoran RB, Ebi H, Turke AB, Coffee EM, Nishino M, Cogdill AP, *et al.* EGFR-mediated re-activation of MAPK signaling contributes to insensitivity of BRAF mutant colorectal cancers to RAF inhibition with vemurafenib. *Cancer Discov* **2012**;2:227–35.

[27] Amodio V, Yaeger R, Arcella P, Cancelliere C, Lamba S, Lorenzato A, *et al.* EGFR blockade reverts resistance to $KRAS^{G12C}$ inhibition in colorectal cancer. *Cancer Discov* **2020**;10:1129–39.

[28] Ryan MB, Fece de la Cruz F, Phat S, Myers DT, Wong E, Shahzade HA, *et al.* Vertical pathway inhibition overcomes adaptive feedback resistance to $KRAS^{G12C}$ inhibition. *Clin Cancer Res* **2020**;26:1633–43.

[29] Kopenhaver J, Crutcher M, Waldman S, Snook A. The shifting paradigm of colorectal cancer treatment: a look into emerging cancer stem cell-directed therapeutics to lead the charge toward complete remission. Expert Opinion on Biological Therapy 2021;21:1335-1345.

[30] Zeuner A, Todaro M, Stassi G, De Maria R. Colorectal cancer stem cells: From the crypt to the clinic. Cell Stem Cell 2014;15:692-705.

[31] Ye ZL, Qiu MZ, Tang T, Wang F, Zhou YX, Lei MJ, *et al.* Gene mutation profiling

in Chinese colorectal cancer patients and its association with clinicopathological characteristics and prognosis. *Cancer Med* **2020**;9:745–56.

[32] Guo F, Gong H, Zhao H, Chen J, Zhang Y, Zhang L, *et al.* Mutation status and prognostic values of KRAS, NRAS, BRAF and PIK3CA in 353 Chinese colorectal cancer patients. *Sci Rep* **2018**;8:6076.

[33] Wang X, Allen S, Blake JF, Bowcut V, Briere DM, Calinisan A, *et al.* Identification of MRTX1133, a noncovalent, potent, and selective $KRAS^{G12D}$ Inhibitor. *J Med Chem* **2022**;65:3123–33.

551 Figure Legends

552 Figure 1. Feedback reactivation of the RAS/MAPK pathway occurs following treatment
553 with sotorasib in colorectal cancer (CRC) cell lines. A) CRC and non-small cell lung
554 cancer (NSCLC) cell lines with various KRAS statuses were treated for 7 h with an
555 increasing concentration of sotorasib, and proliferation was measured by CCK-8 assay.
556 NCI-H358, Calu-1 and NCI-H3122 are NSCLC cell lines, and SW837, SW1463,
557 CACO-2, SW48 and DLD-1 are CRC cell lines. NCI-H358, Calu-1, SE837 and
558 SW1463 have the KRASG12C mutation. B) Cell lines with wild-type KRAS and
559 KRASG12C were treated with sotorasib (1 μM) for 0, 4, and 24 h. Western blot analysis
560 was performed to analyze the expression of proteins related to the EGFR, RAS/MAPK,
561 and PI3K/AKT pathways, and β-actin was used as a loading control.

562

563 Figure 2. Feedback reactivation of the RAS/MAPK pathway occurs following treatment
564 with sotorasib in KRAS gene-transduced CRC cells. Wild-type and mutant KRAS genes
565 (G12C and G12D) were transduced into CACO-2 and SW48, wild-type KRAS CRC
566 cell lines. A) Transduction was confirmed using an anti-FLAG antibody. B) CACO-2
567 and C) SW48 transduced with wild-type and mutated KRAS genes were treated with
568 sotorasib (1 μM) for 0, 4, and 24 h. Western blot analysis was performed to analyze the

569 expression of proteins related to the EGFR, RAS/MAPK, and PI3K pathways, and β-
570 actin was used as a loading control.
571
572
573 Figure 3. Mix culture assay for screening to find therapeutics effective for co-inhibition
574 with sotorasib. A) The relative proliferation rate (RPR) of KRASG12C transduced cells
575 decreased in a concentration-dependent manner of KRASG12C inhibitors. KRASG12C
576 inhibitors selectively reduce RPR with KRASG12C transduced cells. B, C) The RPRs
577 of combination treatment with sotorasib in KRASG12C transduced cells. B) MEK
578 inhibitor enhanced the reduction of the RPR with sotorasib, and the combination
579 treatment of sotorasib and trametinib decreased RPR, specifically in KRASG12C
580 transduced cells. C) Anti-EGFR antibodies induced high RPR in a dose-dependent
581 manner. The combination treatment of sotorasib and cetuximab reduced the RPR in
582 KRASG12C transduced cells. *P<0.05 and **P<0.01.
583
584 Figure 4. MEK inhibitor and anti-EGFR antibody enhance the efficacy of sotorasib. A)
585 CACO-2 and SW48 transduced KRASG12C mutation were treated with sotorasib (1
586 μM), trametinib (1 nM), and/or cetuximab (5 μg/mL) for 24 h, and cell lysate was

587 collected. Western blot analysis was performed to analyze the expression of proteins
588 related to the EGFR and MAPK pathways, and β-actin was used as a loading control. B)
589 CACO-2 and SW48 transduced with wild-type and mutated KRAS were treated with
590 sotorasib (1 μM), trametinib (1 nM), and/or cetuximab (5 μg/mL) for 24 h, and
591 proliferation was assessed by the CCK-8 assay. The combination use of these drugs
592 showed significant growth inhibition to KRASG12C-induced cells. C, D) Sotorasib-
593 resistant and non-resistant cells of CACO-2 transduced KRASG12C mutation were
594 treated with sotorasib (1 μM), trametinib (1 nM), and/or cetuximab (5 μg/mL) for 24 h.
595 Activation of the EGFR and MAPK pathways was analyzed using western blot analysis
596 (C). Proliferation was assessed using the CCK-8 assay (D). *P<0.05 and **P<0.01.
597
598 Figure 5. Combination therapy of sotorasib, trametinib, and cetuximab is effective in
599 vivo. A) KRAS-transduced CACO-2 xenografts were treated with sotorasib (1.0 mg/kg
600 orally once a day) for 21 d. Sotorasib showed a significant effect on tumor reduction
601 compared to the control group in G12C. B) CACO-2 with KRASG12C xenograft
602 treated with sotorasib (0.5mg/kg orally once a day), trametinib (0.05mg/kg orally once a
603 day), cetuximab (50mg/kg intraperitoneally once a week), or combination for 21 d. The
604 three-drug combination significantly inhibited tumor growth compared to the single or

double-drug treatment. C) Immunohistochemistry analysis of KRASG12C-transduced CACO-2 xenograft models. Statistical significance was evaluated compared to the relative size of the 21st day, *P<0.05 and **P<0.01.

Figure1

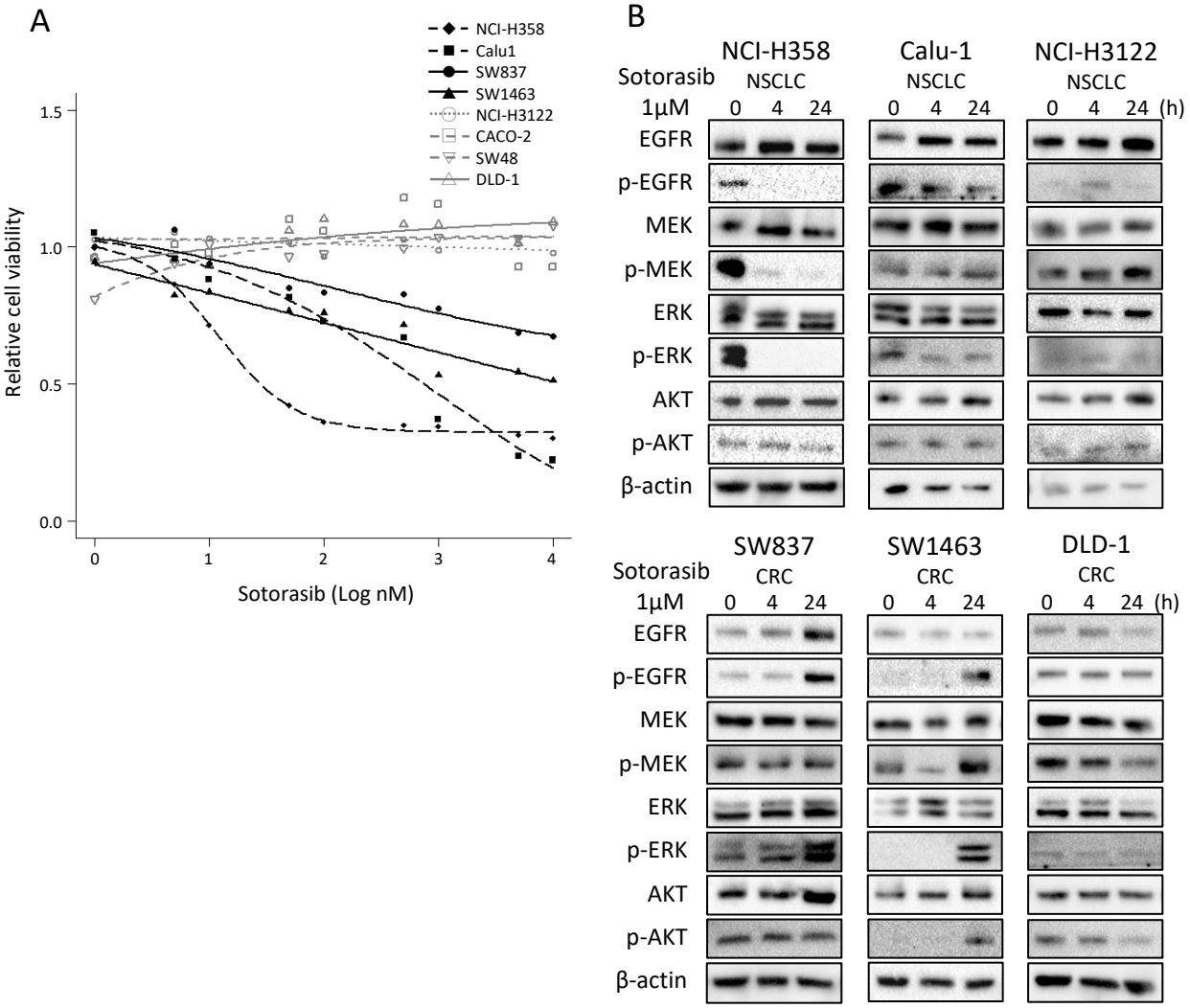
A
NCI-H358
Calu1
SW837
SW1463
NCI-H3122
CACO-2
SW48
DLD-1
Relative cell viability
1.5
1.0
0.5
0.0
0
1
2
3
4
Sotorasib (Log nM)
B
NCI-H358
NSCLC
Calu-1
NSCLC
NCI-H3122
NSCLC
Sotorasib
1μM
0 4 24
0 4 24
0 4 24 (h)
EGFR
p-EGFR
MEK
p-MEK
ERK
p-ERK
AKT
p-AKT
β-actin
SW837
CRC
SW1463
CRC
DLD-1
CRC
Sotorasib
1μM
0 4 24
0 4 24
0 4 24 (h)
EGFR
p-EGFR
MEK
p-MEK
ERK
p-ERK
AKT
p-AKT
β-actin

Figure2

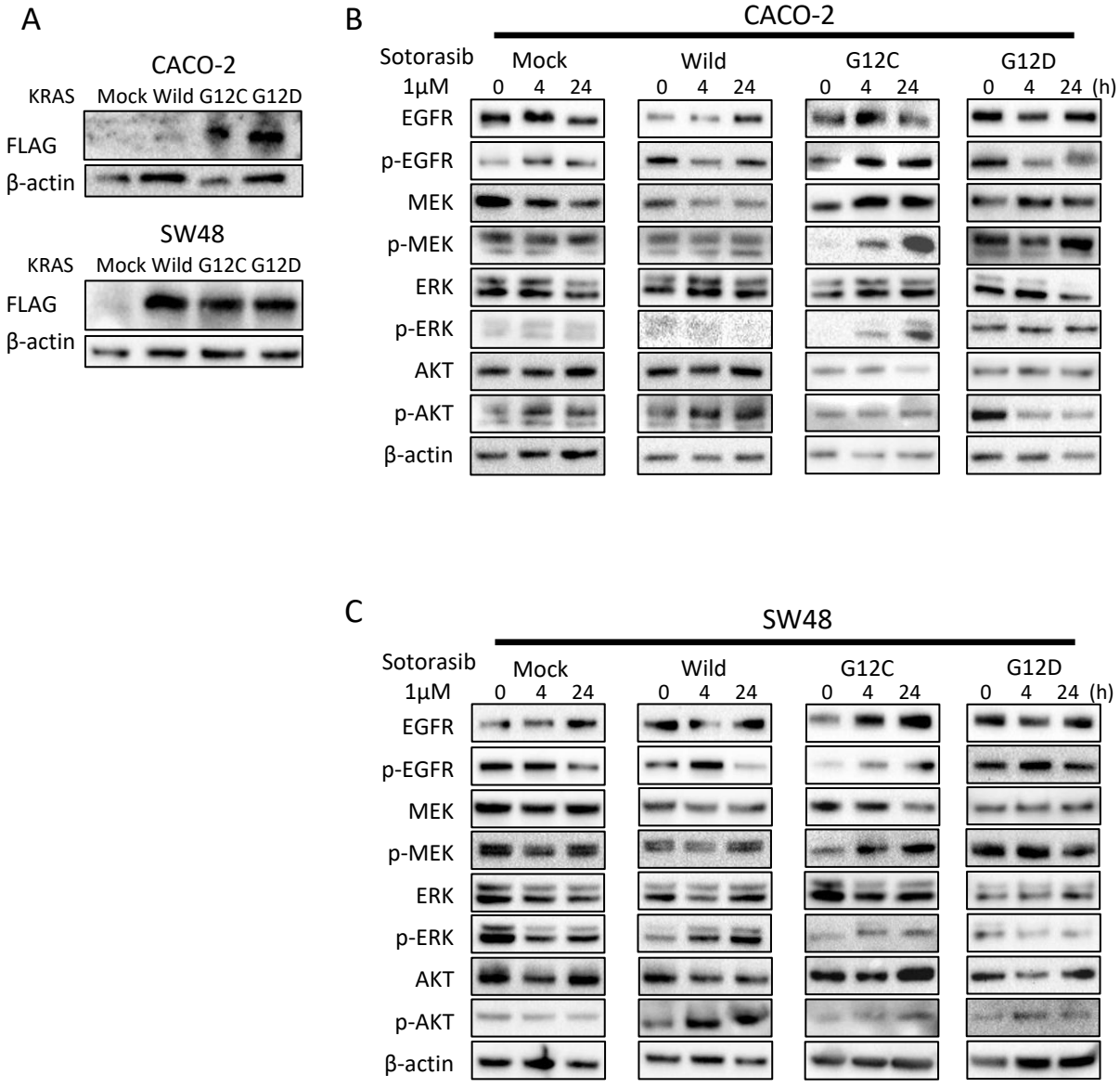
A
CACO-2
KRAS Mock Wild G12C G12D
FLAG
β-actin
SW48
KRAS Mock Wild G12C G12D
FLAG
β-actin
B
CACO-2
Sotorasib 1μM
Mock
Wild
G12C
G12D
0 4 24 (h)
EGFR
p-EGFR
MEK
p-MEK
ERK
p-ERK
AKT
p-AKT
β-actin
C
SW48
Sotorasib 1μM
Mock
Wild
G12C
G12D
0 4 24 (h)
EGFR
p-EGFR
MEK
p-MEK
ERK
p-ERK
AKT
p-AKT
β-actin

Figure3

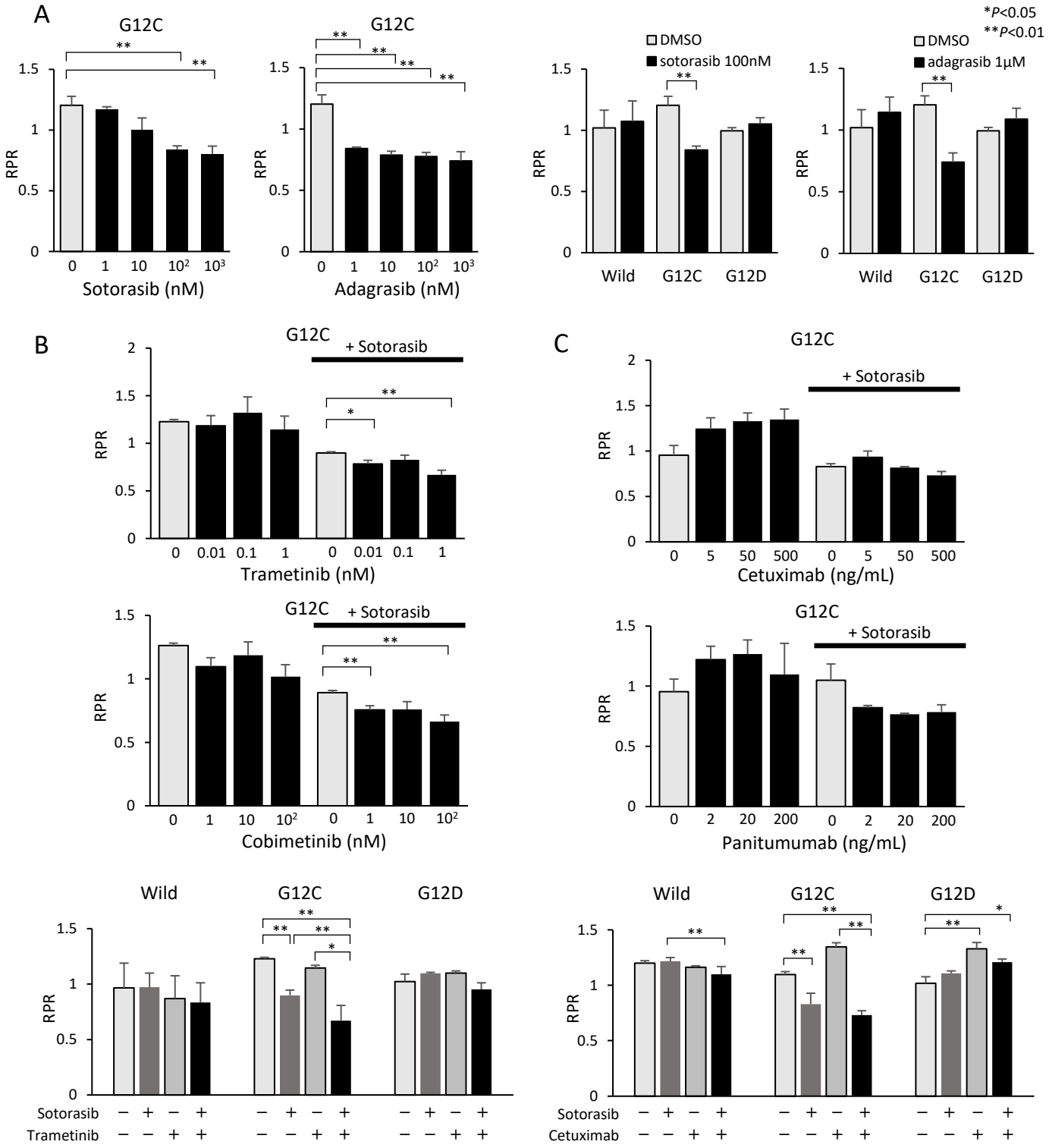
A
G12C
RPR
Sotorasib (nM)
Adagrasib (nM)
*P<0.05
**P<0.01
DMSO
sotorasib 100nM
adagrasib 1μM
Wild
G12C
G12D
B
+ Sotorasib
Trametinib (nM)
Cobimetinib (nM)
C
Cetuximab (ng/mL)
Panitumumab (ng/mL)
Sotorasib
Trametinib
Cetuximab

Figure4

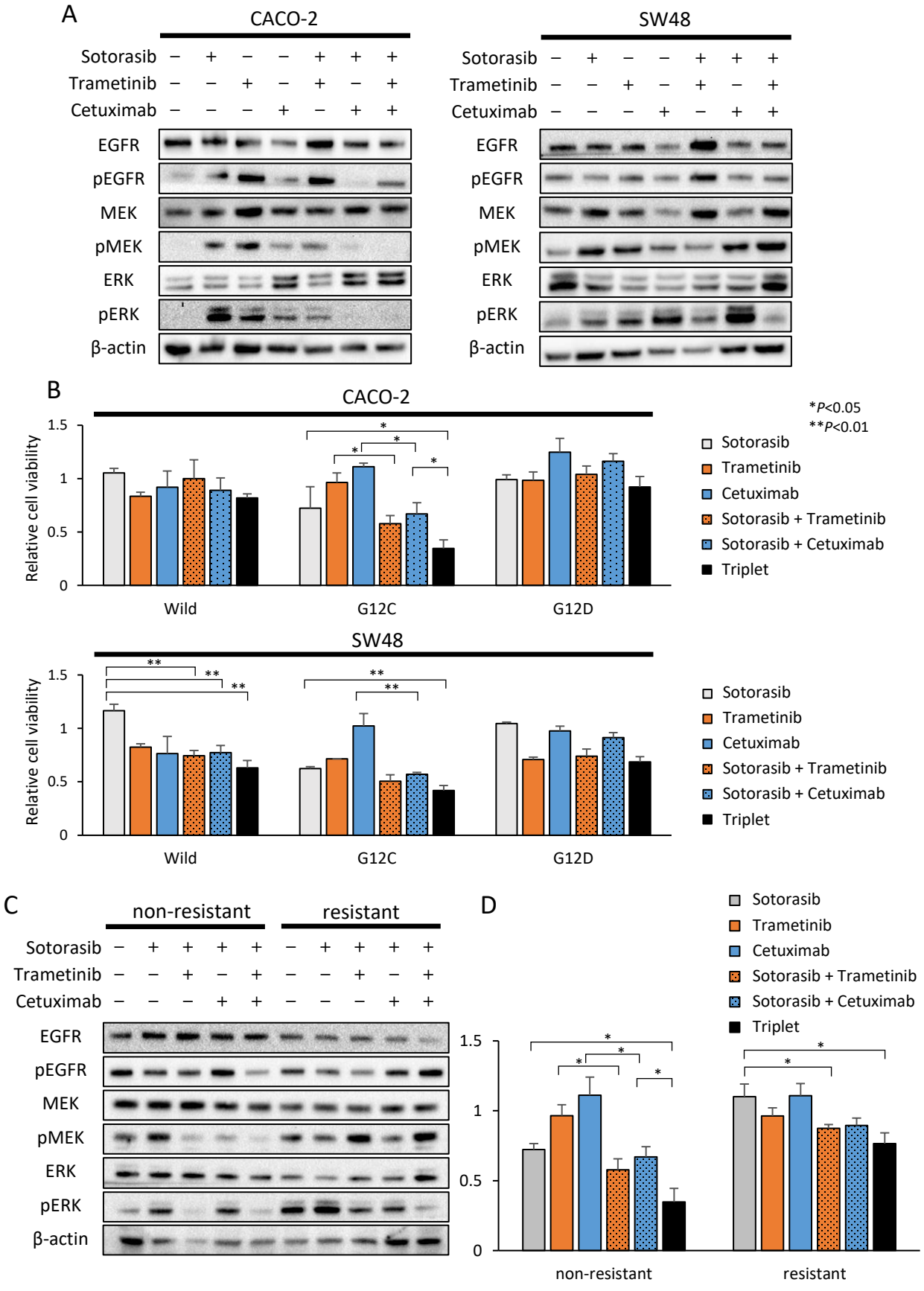
A
CACO-2
SW48
Sotorasib
Trametinib
Cetuximab
EGFR
pEGFR
MEK
pMEK
ERK
pERK
β-actin
B
CACO-2
SW48
Relative cell viability
Wild
G12C
G12D
*P<0.05
**P<0.01
Sotorasib
Trametinib
Cetuximab
Sotorasib + Trametinib
Sotorasib + Cetuximab
Triplet
C
non-resistant
resistant
D
non-resistant
resistant

Figure5

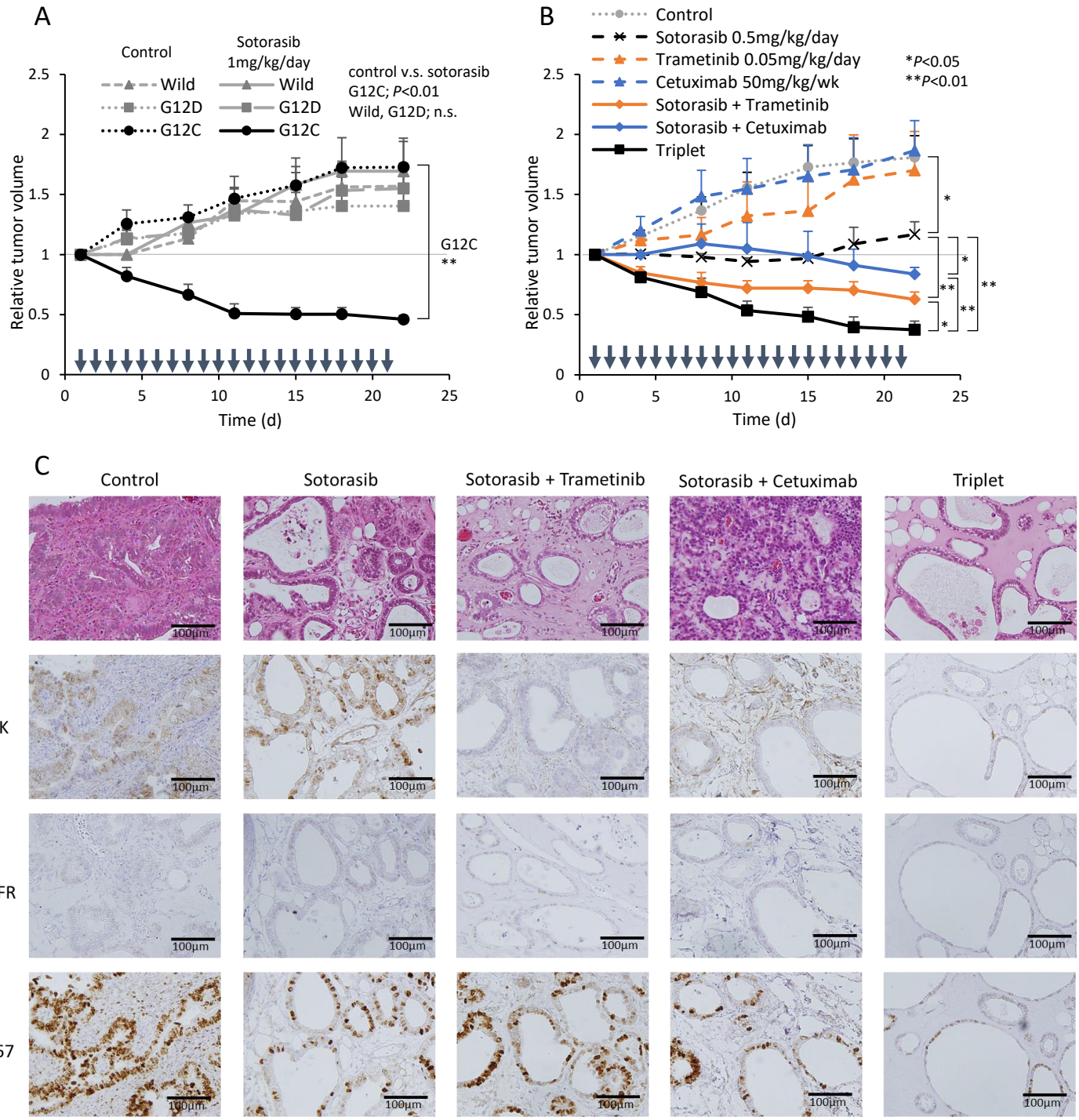
A
Control
Sotorasib 1mg/kg/day
Wild
G12D
G12C
control v.s. sotorasib
G12C; P<0.01
Wild, G12D; n.s.
G12C **
Relative tumor volume
Time (d)
B
Control
Sotorasib 0.5mg/kg/day
Trametinib 0.05mg/kg/day
Cetuximab 50mg/kg/wk
Sotorasib + Trametinib
Sotorasib + Cetuximab
Triplet
*P<0.05
**P<0.01
Relative tumor volume
Time (d)
C
Control
Sotorasib
Sotorasib + Trametinib
Sotorasib + Cetuximab
Triplet
HE
pERK
pEGFR
Ki-67
100μm

Supplementary Table S1

Relative cell viability of each cell lines with $KRAS^{G12C}$

Relative cell viability (5μM of sotorasib)		*p* value	
NCI-H358	0.31 ±0.02	0.0167(vs SW837)	>0.001(vs SW1463)
Calu-1	0.24 ±0.05	0.0108(vs SW837)	>0.001(vs SW1463)
SW837	0.69 ±0.11		
SW1463	0.54 ±0.03		

Colorectal cancer (CRC) and non-small cell lung cancer (NSCLC) cell lines with $KRAS^{G12C}$ were treated for 72 h with 5 μM of sotorasib, and the proliferation was a by CCK-8 assay. The relative cell viability of each cell was shown. The cell viability was compared between NSCLC and CRC cells.

Supplementary Figure S1

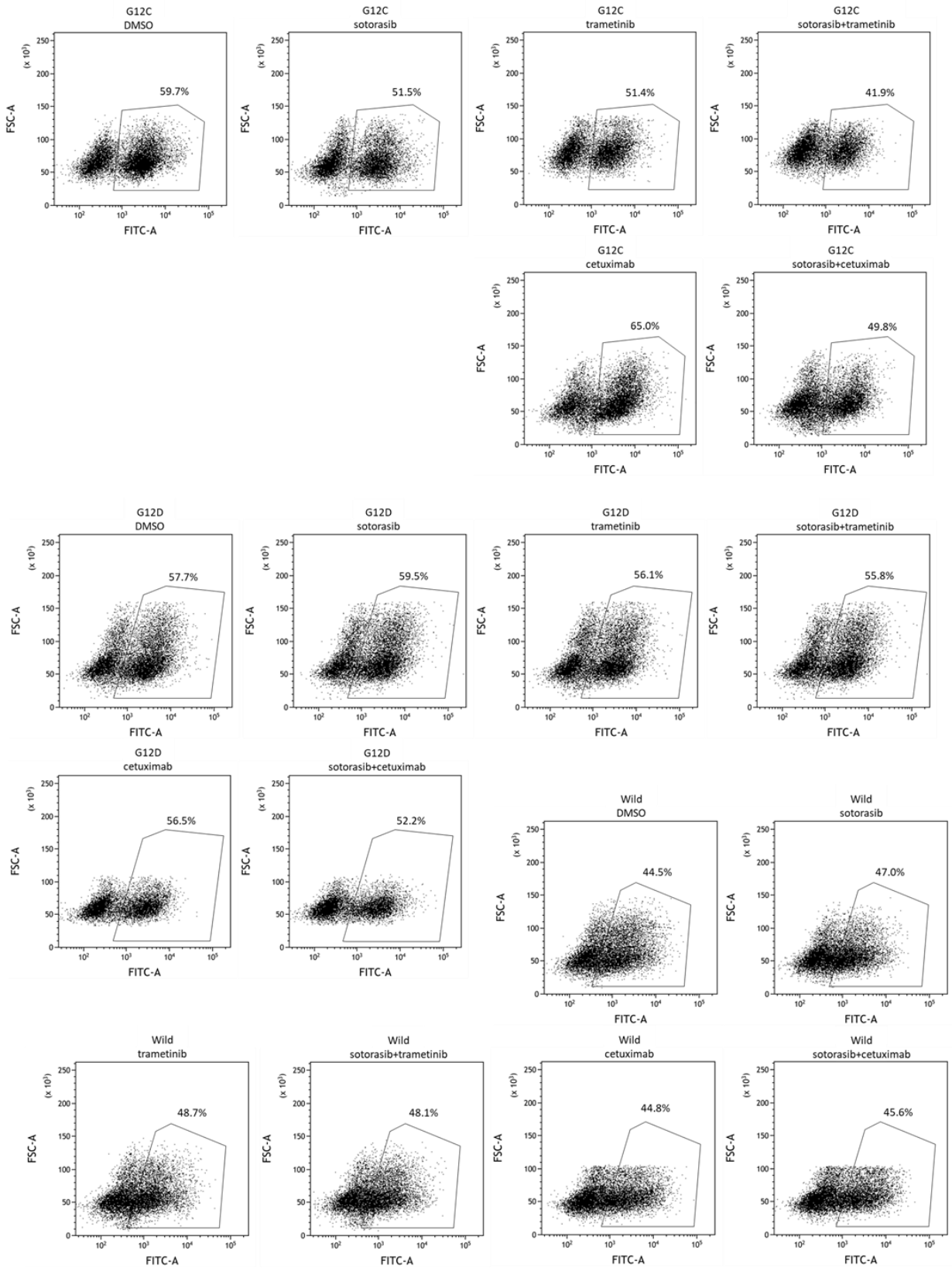

The plots of flow cytometry experiments. The GFP-positive ratio after treatment with sotorasib, trametinib, and/or cetuximab.

Supplementary Figure S2

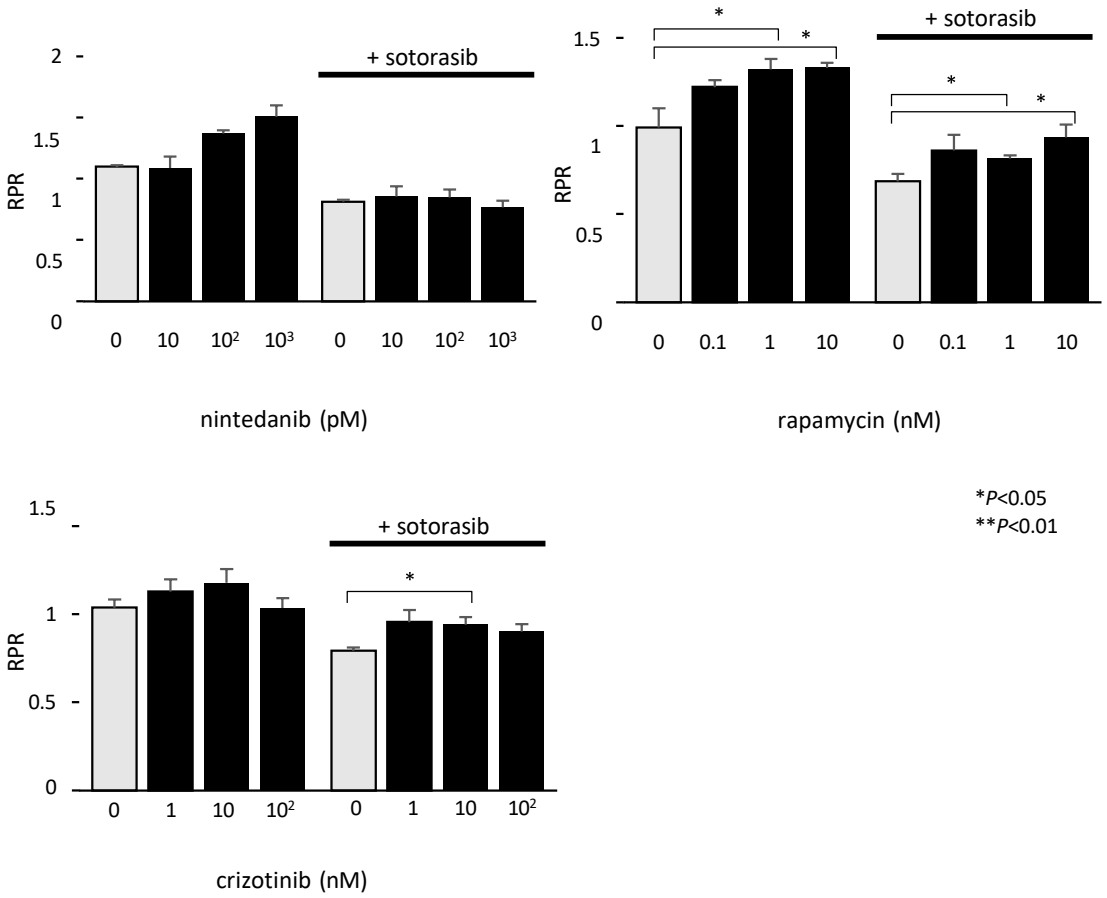

Mix culture assay for screening of effective therapeutics for co-inhibition with sotorasib. These drugs did not decrease the relative proliferation rate (RPR) when combined with sotorasib.

Supplementary Figure S3

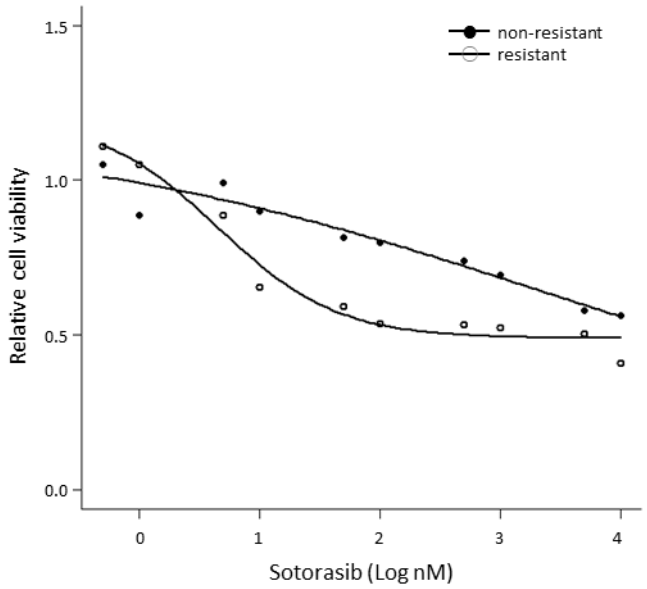

We established sotorasib-resistant and non-resistant cell lines of KRASG12C-transduced CACO-2 cells. The drug sensitivity of sotorasib is shown.

Supplementary Figure S4

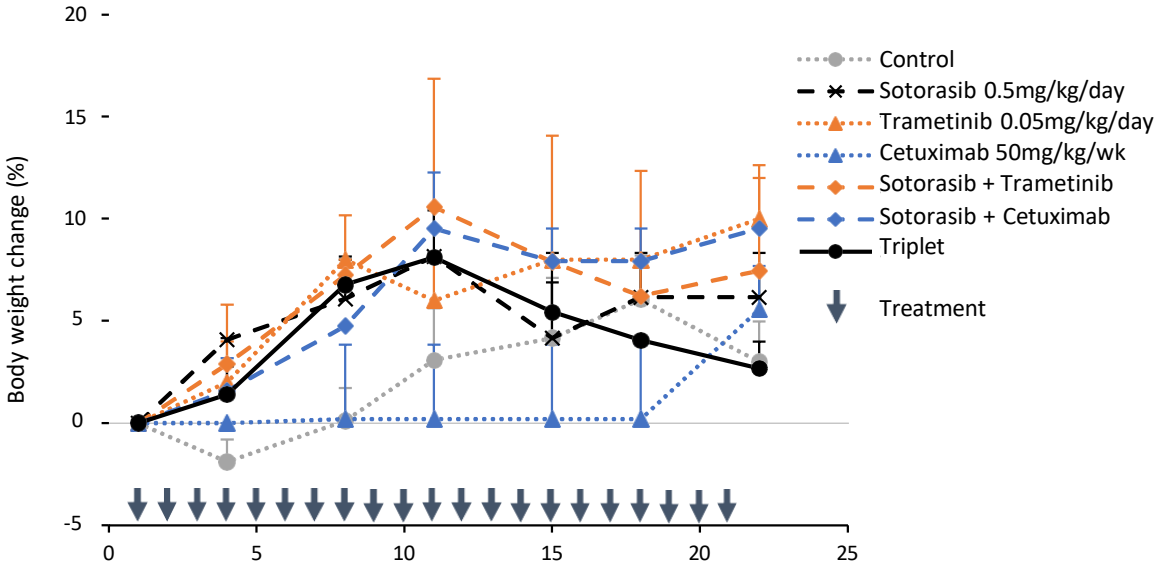

The body weight changes of CACO-2 with KRAS^{G12C} xenograft mice during combined treatments.